The embryonic expression patterns of zebrafish genes encoding LysM-domains

Laroche, F.J.F.; Tulotta, C.; Lamers, G.E.M.; Stougaard, J.; Blaise, M.; Verbeek, F.J.; ... ; Spaink, H.P.

Gene Expression Patterns 13 (2013) 212–224

Contents lists available at SciVerse ScienceDirect

Gene Expression Patterns

journal homepage: www.elsevier.com/locate/gep

The embryonic expression patterns of zebrafish genes encoding LysM-domains

F.J.F. Laroche [a,b,*], C. Tulotta [b], G.E.M. Lamers [b], A.H. Meijer [b], P. Yang [c], F.J. Verbeek [c], M. Blaise [a], J. Stougaard [a], H.P. Spaink [a,b]

[a] Centre for Carbohydrate Recognition and Signalling, Department of Molecular Biology and Genetics, Aarhus University, Gustav Wieds vej 10, 8000 Aarhus C, Denmark
[b] Leiden University, Institute of Biology, Molecular Cell Biology Department, Leiden University, Einsteinweg 55, 2333 CC Leiden, The Netherlands
[c] Leiden Institute for Advanced Computer sciences (LIACS), Leiden University, Niels Borhweg 1, 2333 CA Leiden, The Netherlands

ARTICLE INFO

Article history:
Received 18 December 2012
Received in revised form 14 February 2013
Accepted 21 February 2013
Available online 6 April 2013

Keywords:
LysM domains
TLDc domains
OXR
CNS
Zebrafish

ABSTRACT

The function and structure of LysM-domain containing proteins are very diverse. Although some LysM domains are able to bind peptidoglycan or chitin type carbohydrates in bacteria, in fungi and in plants, the function(s) of vertebrate LysM domains and proteins remains largely unknown. In this study we have identified and annotated the six zebrafish genes of this family, which encode at least ten conceptual LysM-domain containing proteins. Two distinct sub-families called LysMD and OXR were identified and shown to be highly conserved across vertebrates. The detailed characterization of LysMD and OXR gene expression in zebrafish embryos showed that all the members of these sub-families are strongly expressed maternally and zygotically from the earliest stages of a vertebrate embryonic development. Moreover, the analysis of the spatio-temporal expression patterns, by whole mount and fluorescent *in situ* hybridizations, demonstrates pronounced LysMD and OXR gene expression in the zebrafish brain and nervous system during stages of larval development. None of the zebrafish LysMD or OXR genes was responsive to challenge with bacterial pathogens in embryo models of *Salmonella* and Mycobacterium infections. In addition, the expression patterns of the OXR genes were mapped in a zebrafish brain atlas.

1. LysM domain encoding genes and proteins

1.1. Diversity among LysM domain containing proteins

LysM domain containing proteins are very diverse and widely studied in bacteria, fungi and plants. In several bacteria (Buist et al., 2008) LysM containing proteins are involved in peptidoglycans (PGN) synthesis and in catabolic processes modifying the cell wall. A peptidoglycan hydrolase, AcmA, the N-acetyl-glucosaminidase from *Lactococcus lactis*, is a typical example of a bacterial LysM-domain containing protein. Very diverse groups of LysM domain containing peptidases, reductases, nucleotidases, chitinases or esterases are represented in bacterial proteomes. The LysM domains of AcmA were shown (Steen et al., 2005) to be responsible for binding the carbohydrate of PGN.

In legumes, kinase proteins carrying multiple LysM domains in their extracellular domains enable the host plant to recognize signal molecules secreted by symbiotic bacteria. In the model legume *Lotus japonicus* the two receptor kinases, NFR1 and NFR5, are required for perception of lipo-chito-oligosaccharide (Nod factors) signal molecules secreted by the symbiotic bacteria. The LysM2 domain of NFR5 was shown to be involved in deciphering the Nod factor structure (Madsen et al., 2003; Radutoiu et al., 2003, 2007). More recently direct high-affinity binding of Nod factor by the NFR1 and NFR5 receptors was demonstrated (Broghammer et al., 2012). Other LysM-domain protein kinases sense and induce resistance against fungi by perception of chitin molecules secreted by the pathogen (Wan et al., 2008). Two LysM proteins, *CERK1* and *CEBiP*, are involved in chitin signalling and host defence response in rice or in the model plant *Arabidopsis thaliana* (Miya et al., 2007; Shimizu et al., 2010). During fungal infection of tomato the *Cladosporium fulvum* pathogen secretes a LysM protein, called Ecp6, into the intercellular space. Ecp6 prevents tomato immune response by sequestering chitin oligosaccharides that are released from fungal cell walls (de Jonge et al., 2010). Direct binding of plant LysM proteins was also found with peptidoglycans (Willmann, 2012) (PGN). The LYM1/LYM3/CERK1 perception system (composed of three LysM domain containing proteins) is involved in PGN sensing and leads to an immune response (Willmann, 2012).

1.2. Animal LysM domain containing proteins

Only a few studies have addressed the function of animal LysM-domain containing proteins. From the human genome, a

* Corresponding author at: Centre for Carbohydrate Recognition and Signalling, Department of Molecular Biology and Genetics, Aarhus University, Gustav Wieds vej 10, 8000 Aarhus C, Denmark. Tel.: +31 715274950; fax: +31 715275088.
E-mail address: f.laroche@biology.leidenuniv.nl (F.J.F. Laroche).

1567-133X/$ - see front matter © 2013 Elsevier B.V. All rights reserved.
http://dx.doi.org/10.1016/j.gep.2013.02.007

LysM-domain encoding gene was originally identified while screening for oxidation resistance genes. Based on the observed reversion of a mutated phenotype in a prokaryotic oxidative mutagenesis assay, the gene was named oxidation resistance 1 (*OXR1*)Volkert et al., 2000. Later, the OXR family of genes was expanded (Durand et al., 2007) with *OXR2*, another LysM domain encoding gene providing resistance to oxidation (Durand et al., 2007) highly similar to *OXR1*. The minimal oxidation resistance domain found in the OXR family of proteins was associated (Murphy et al., 2012) with the region encoded by exon8. Recently the mouse OXR1 protein was shown as a novel neuro-protective factor both *in vitro* and *in vivo* (Oliver et al., 2011). *OXR2* was first isolated (Shao et al., 2002) in a screening for Estrogen Receptor (ER) interacting proteins using an Akata Burkitt's lymphoma cell cDNA library. The protein was originally named ER Activating Protein of 140 kDa and classified (Shao et al., 2002) in the Nuclear Co-Activator family (*ERAP140*) because of this affinity with ER. In addition to the interaction with ERα, hOXR2 protein has affinity for ERβ, thyroid hormone receptor beta (TRβ), peroxisome proliferator-activated receptor gamma (PPARγ), and retinoic acid receptor alpha (RARα). The characterization of these interactions suggested that *OXR2* represents a distinct class of nuclear receptor co-activators (Shao et al., 2002) (NCOA7). Steroid hormone receptors like ER or Androgen Receptor (AR) are sensing proteins that control important biological processes and therefore *OXR2* gene activity has been studied in this context. Transcriptome studies (Kinyamu et al., 2009) in MCF-7 breast cancer cells show increased *OXR2* expression upon proteasomal inhibition with MG132 (epoxomycin). However, *OXR2* was not regulated (Kinyamu et al., 2009) in MCF-7 cells treated with 17β-estradiol. Silencing of *OXR2* with siRNA in an androgen responsive prostate cancer cell line (LNCaP PCa cells) decreased AR expression and led to a marked difference in the androgen responsiveness of genes involved in prostate cancer (Heemers et al., 2009). The human *OXR2* gene (*NCOA7*) was suggested as a potential pharmaceutical target for the treatment of prostate cancer (Heemers et al., 2009). In addition, a high expression level of *OXR2* was reported as a novel, favourable, prognostic indicator for neuroblastoma (Arai et al., 2008). Moreover it was recently proposed that genetic variants of *OXR2* may confer a reduced risk of breast cancer (Higginbotham et al., 2011).

At least two genetic mapping studies point toward a linkage between the human *OXR2* locus (6q22) and families with bipolar disorders (Middleton et al., 2004; Pato et al., 2005). Consequently, the role of *OXR2* in schizophrenia spectrum disorders was investigated. An independent study did not associate schizophrenia with any of the six polymorphisms within the *OXR2* sequence (Liu et al., 2007). However overlapping *de novo* interstitial micro-deletions involving the human *LysMD3* locus (5q14.3-q15), demonstrated with molecular karyotyping and fluorescence *in situ* hybridizations (DNA FISH), connect *LysMD3* to symptoms of psychomotor retardation and brain anomalies (Engels et al., 2009). Furthermore, at least one study (Thisse et al., 2004) have shown that *LysMD3* and *LysMD2* are expressed during early zebrafish embryonic developmental stages. These studies indicate that LysM domain encoding genes may play a role in brain and in nervous system development and functioning. Presently, no LysM family member has been clearly associated with any human disease and no vertebrate knockout model is available.

1.3. Research strategies

In this report we identify the LysM domain encoding genes from zebrafish and compare those with their human orthologs. In addition we describe two sub-families of LysM encoding genes consisting of *OXR1*, *OXR2* (OXR genes) and *LysMD1* to *LysMD4* (LysMD genes). Ten different LysM domain encoding cDNAs were cloned from zebrafish embryos and six LysM domain genes encoding eight LysM-domain containing proteins were annotated. We searched micro-arrays data sets, for the LysM family genes regulations in response to *Mycobacterium marinum* and *Salmonella typhimurium* infections in zebrafish embryos, and performed spatio-temporal study of LysM encoding gene expression during zebrafish embryonic development, as first steps to elucidate their function. The brain and nervous system expression patterns were demonstrated at 48 hours post fertilization (hpf) by comparing *OXR2* WISH stained micro-sections with laser fluorescence scanning confocal stacks, from *OXR2* fluorescence *in situ* hybridizations (RNA FISH). Moreover *OXR1* and *OXR2* expression patterns were modelled in three dimensions and these datasets were integrated into software dedicated to the zebrafish brain atlas.

2. Results

2.1. The gene families encoding LysM-domain containing proteins in zebrafish

Using the Conserved Domain Database (CDD) tool (NCBI), representatives of two different sub-families of LysM-domain containing proteins can be found in several animal genomes. We used a LysM-domain consensus of 44 amino acids (aa) (Pfam PFO1476) and representatives of these sub-families to search the zebrafish databases (BLAST and TBLASTN) and identified six different LysM-domain encoding genes in the zebrafish genome (shown in Fig. 1, Panel A: LysMD; Panel B: OXR). Subsequent cloning and sequencing of cDNAs isolated by RT-PCR from wild type zebrafish embryos revealed expression of these six genes, as well as alternative splicing into at least ten transcripts corresponding to eight different LysM domain containing proteins. However, as alternative splicing frequently occurs in zebrafish, this list of LysM encoding cDNAs and putative protein isoforms is not exhaustive. The primer sequences used for cloning LysM encoding cDNAs are given in Supplementary Table 1.

2.1.1. The zebrafish LysMD sub-family of LysM encoding genes

The zebrafish LysMD genes have a similar architecture with only three exons spanning a short genetic distance (maximum 15 kb). The LysMD genes encode relatively small proteins of no more than 305 amino acids (Fig. 1, Panel A). Homology domain analysis of the translated LysMD cDNA sequences identified a single LysM domain in the LysMD1, LysMD2, LysMD3 and LysMD4 proteins. One cDNA alternatively spliced from *LysMD2* contains an open reading frame (ORF) of 88 aa but was not predicted to contain any homology domain within its sequence. Single pass transmembrane domains were predicted from both *LysMD3* and *LysMD4* sequences. No other domains were predicted from the LysMD sequences cloned from zebrafish.

In zebrafish the *LysMD1* locus on Chr16 was represented by a single transcript composed of three exons encoding a 211 aa protein with a single LysM domain. The *LysMD2* locus located on Chr18 was represented by two different splice variants. The first variant was composed of three exons encoding a 208 aa LysM-domain containing protein named LysMD2A. The second variant named LysMD2B is a polypeptide of 88 aa. LysMD2B cDNA (BankIt1447130 LysMD2B accession number JQ686226) contains only exon one directly followed by exon three and shows alternative splicing of exon two, leading to a stop codon instead of a methionine in exon three. The *LysMD3* locus on Chr5 gives rise to at least one transcript composed of three exons encoding a 305 aa polypeptide with a predictable single pass trans-membrane domain in its Ct region (*TOPRED* 0.01 and THMM predictions). The *LysMD4* locus is on Chr18 and is transcribed into at least one transcript

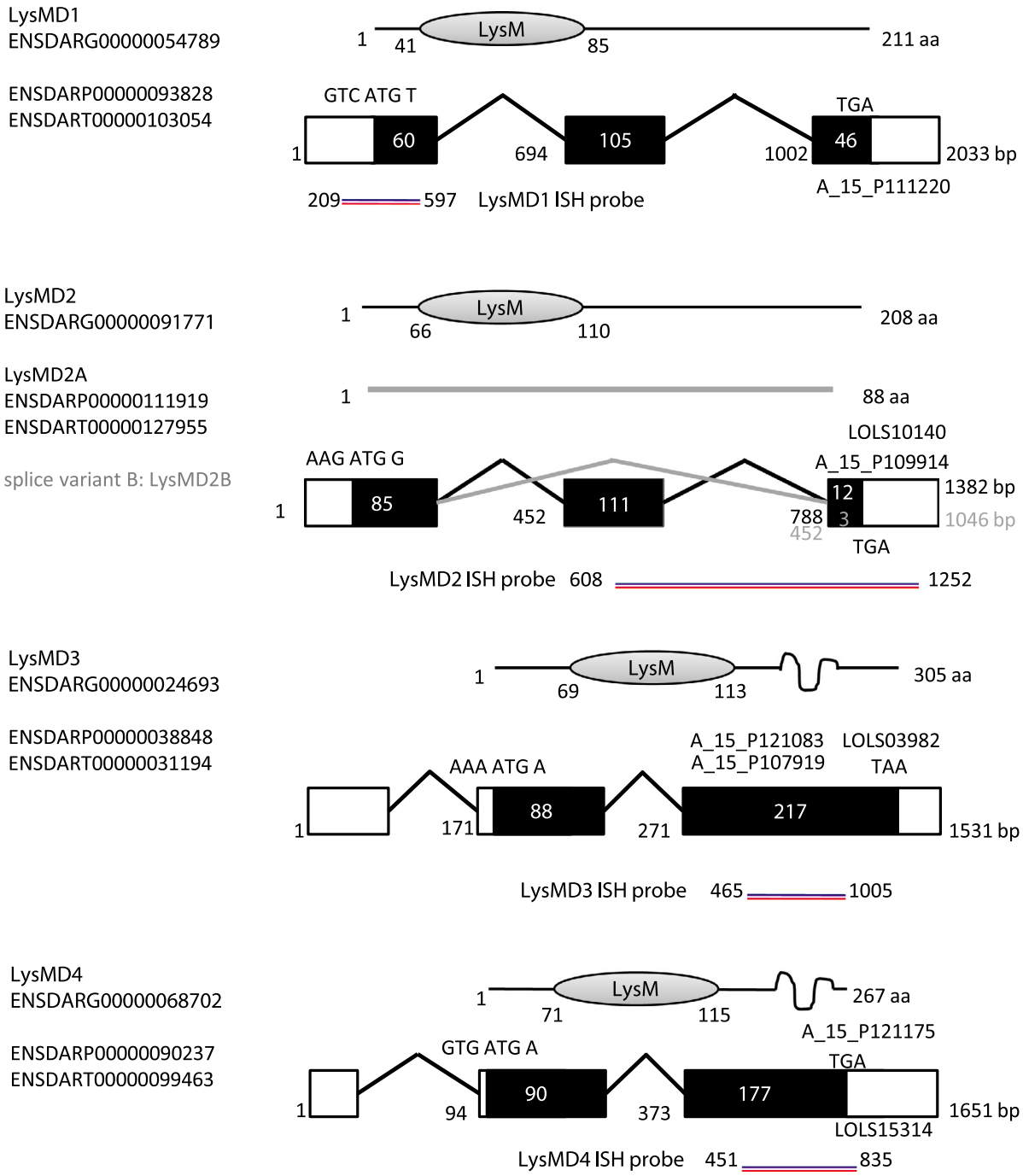

Fig. 1. Schematic representation of LysMD (panel A) and OXR (panel B) genes and proteins. Black exons are coding protein sequences and white exons are 5' or 3' untranslated sequences (UTR). The number inside each black box represents the number of amino acids encoded in each exon. Small numbers at the bottom of each exon indicate the location of each exon inside a transcript sequence (in base pair). Kozak ribosomal binding sequences (RBS) are reported at the translational start site and stop codons are indicated. *In situ* hybridization probes are drawn in blue/red lines for each transcript. Microarray probes are shown at their hybridization locus. These schemes are not drawn to scale.

encoding a 267 aa protein. A trans-membrane domain can be predicted in LysMD4 Ct region (TOPRED 0.01 and THMM prediction).

2.1.2. The zebrafish OXR sub-family of LysM encoding genes

With gene architectures covering over 90 Kb, the zebrafish OXR genes span much larger genetic distances than the LysMD genes. In addition to a single LysM domain, bioinformatic analysis of the zebrafish and human proteins predicted a GRAM domain and a TLDc homology domain from zebrafish *OXR1* and *OXR2* cDNAs. The function(s) of TLDc domains is currently unknown although the TLDc domain also occurs in TBC containing proteins. Recently the TLDc domain encoded in zebrafish *OXR2* was purified and crystallised (Alsarraf et al., 2011) and structural analysis revealed a new protein domain fold (Blaise et al., 2012). The GRAM homology domain is found in glucosyl-transferases, in myotubularins and in other membrane associated proteins (Dorrks et al., 2000). The GRAM domain of the human OXR1 protein was associated (Murphy and Volkert, 2012) with the oxidation resistance effect. Mutation in the GRAM domain of myotubularins is a cause of myopathy (Tsujita et al., 2004). This information suggests that the GRAM domain is required for full functionality of OXR1. GRAM is proposed to be an intracellular protein-binding or lipid-binding sensing do-

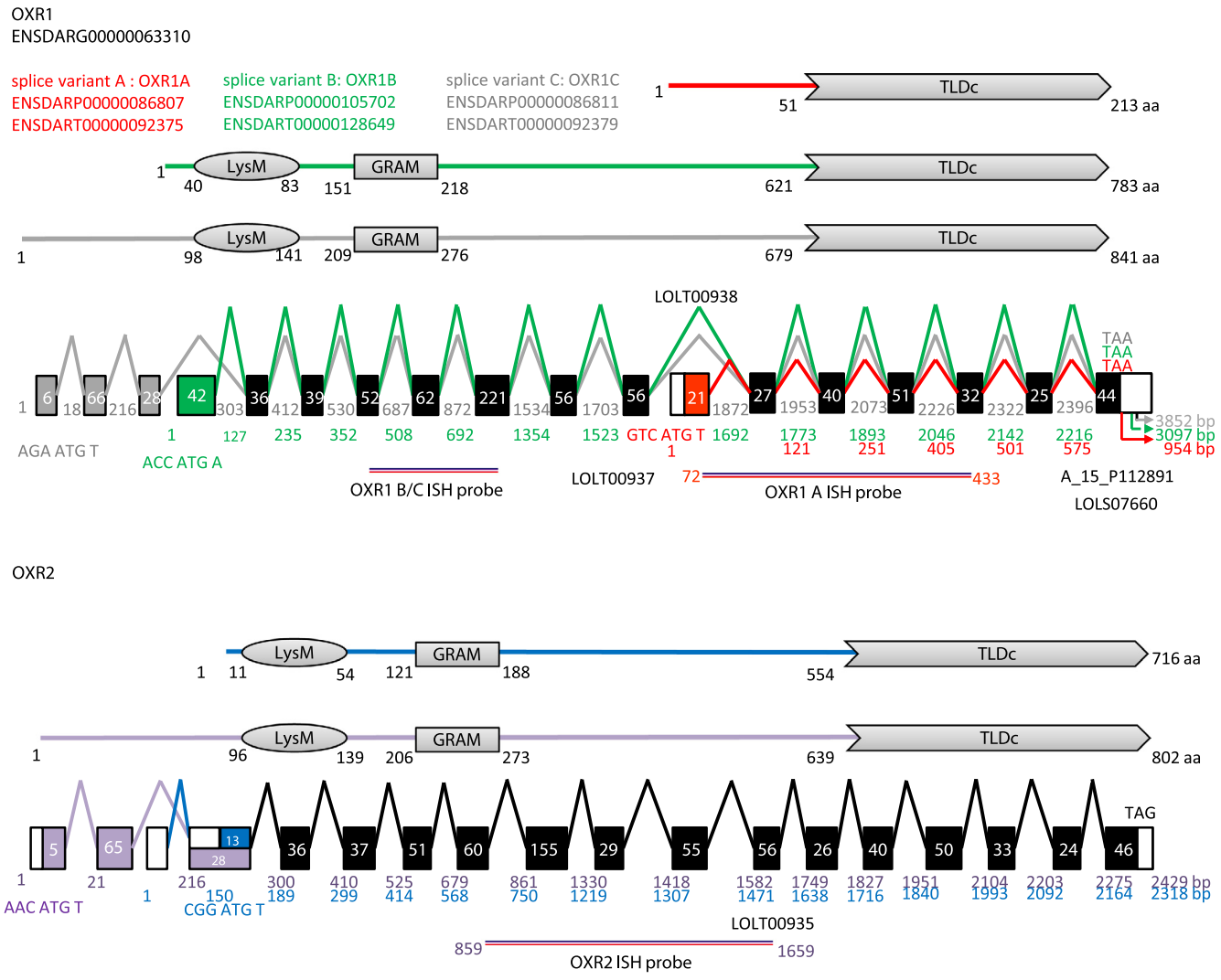

Fig. 1. (*continued*)

main, which has an important function in membrane-associated processes (Doerks et al., 2000).

The *OXR1* locus is on Chr19 and this gene is composed of at least 18 exons (Fig. 1; Panel B). Alternatively spliced transcripts represented by three different cloned cDNAs were named OXR1A, OXR1B and OXR1C. The first exon was found only in OXR1C and appears specific to the longest splice variant of OXR1C, containing 841 aa. Exon four encodes 42 aa and is found only in the 783 aa OXR1B protein. Exon twelve is found only in the shortest OXR1 transcript that we call OXR1A, corresponding to a polypeptide of 213 aa and predicted to contain only the TLDc domain. In addition, we obtained RT-PCR evidence for the existence of an alternative transcript specific 3′ untranslated region (UTR) in *OXR1* (drawn in Fig. 1, Panel B. *OXR1*); OXR1C is the longest transcript with the longest 3′UTR, while OXR1A is the shortest transcript and has the shortest 3′UTR. In zebrafish *OXR2* is found on Chr16 and gives rise to at least two transcripts, composed of eighteen exons, encoding two conceptual proteins that we proposed as OXR2A (accession number: JQ649325) and OXR2B (accession number: JQ649326) (drawn in Fig. 1, Panel B).

2.1.3. LysMD and OXR phylogeny

Representatives of LysMD and OXR protein families are found among all vertebrates studied, also in insects like the fruit fly and even in an amibea transcriptome (*Dictyostelium Discoidum*). In the fruit fly genome *Drosophila Melanogaster*, at least four LysM encoding genes are found in clusters with LysMD and OXR. One well annotated LysM encoding gene clustering with an OXR gene (previously known as *L82* (Stowers et al., 1999) was recently renamed mustard (Mtd) Wang et al., 2012. The *L82* has twenty annotated transcripts, twenty known polypeptides and 23 reported alleles. The longest isoform, 82Fd-RV, encodes both a LysM domain and TLDc domains and all spliced forms contain a Ct region that corresponds with the TLDc domain. *L82* does not appear to encode any GRAM domain but 82Fd-RV contains two TLDc domains in a row. Knocking down *L82* leads to developmental delay and lethality at eclosion that is caused by a failure to release the fruit fly from the pupal case (Stowers et al., 1999). The mustard gene (Mtd) appears able to alter the innate immune response from the fly toward *Vibrio cholerae* (Wang et al., 2012). Wang and collaborators suggest (Wang et al., 2012) the small *Mtd* homologs from vertebrate OXR1 and NCOA7 may have a similar function. They present evidence to suggest the fly eclosion defect that was previously attributed to the *L82* locus may result from unopposed action of *NF-KB* fly homologs. In the mosquito *Anopheles gambiae*, Jaramillo-Gutierrez and collaborators have shown (Jaramillo-Gutierrez et al., 2010) the involvement of an OXR family member in a JNK regulated pathway acting on catalase and glutathione peroxidase mRNA levels, which

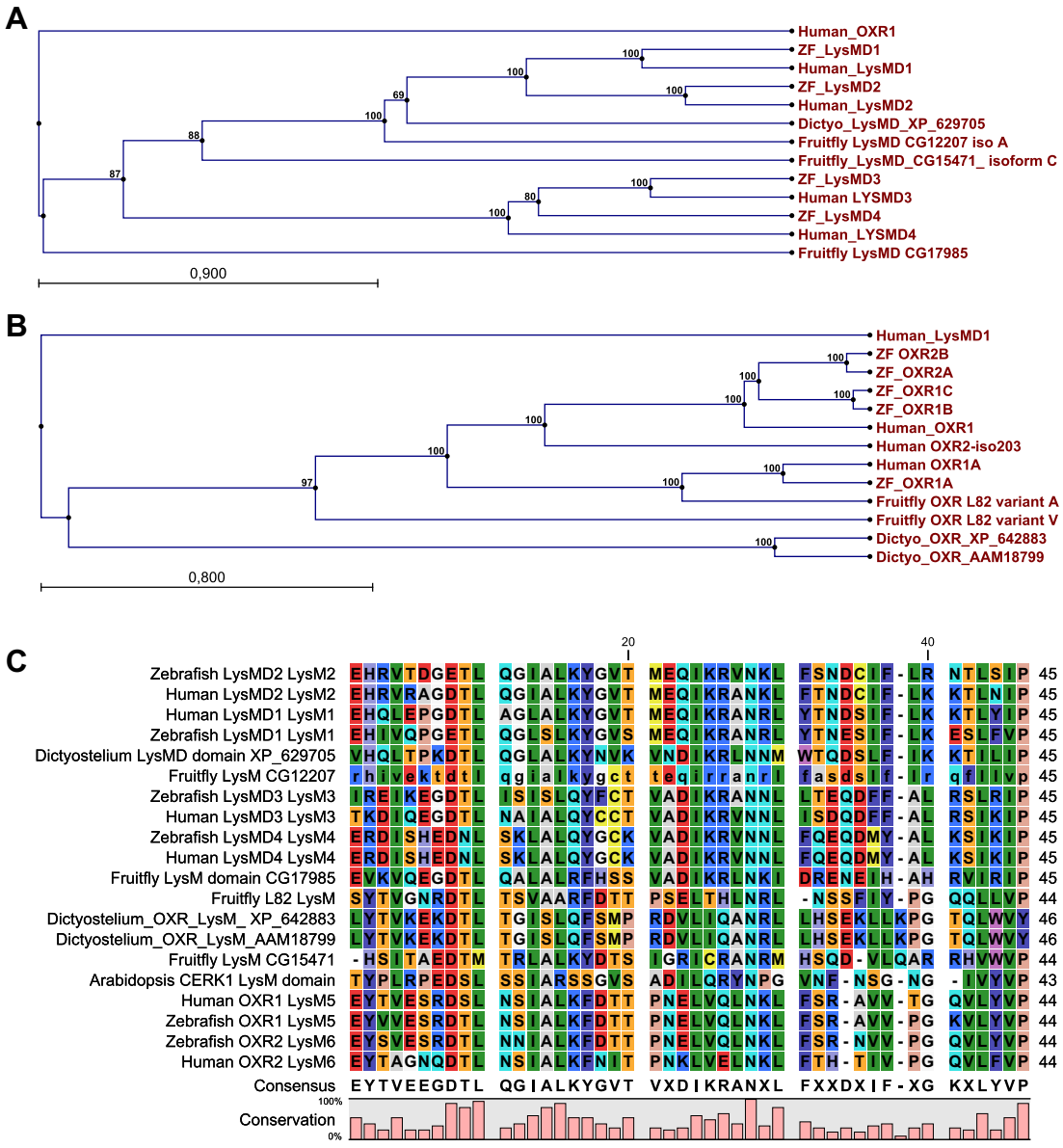

Fig. 2. Phylogenetic trees comparing full length LysM encoding proteins (LysMD in panel A and OXR in panel B). Numbers indicate bootstrap values between respective orthologs. Branch nexus are marked with a dot and indicates probable common ancestry for a subgroup of full length LysM domain containing proteins. A minimal LysM domains amino acids pairwise alignment is displayed in panel C. The minimal LysM domains sequences were obtained with SMART.

are the main detoxifying enzymes of the cell. The mosquito is the main vector of malaria disease in vertebrate hosts and silencing *OXR1* decreases *Plasmodium* infection in the mosquito, while silencing *JNK* increases *Plasmodium* amounts in mosquito blood (Jaramillo-Gutierrez et al., 2010). Both *OXR1* and *JNK* appear to be required for mosquito females to survive chronic oxidative stress treatments (Jaramillo-Gutierrez et al., 2010).

Phylogenetic trees comparing full length LysMD and OXR proteins from zebrafish to those from humans are presented (Fig. 2, panel A and panel B). The LysMD1 and LysMD2 proteins cluster together whilst in a different branch LysMD3 clusters with LysMD4. These two LysMD branches have a common nexus. The zebrafish LysMD and OXR proteins and their human orthologs appear relatively conserved in this analysis. Supporting this common ancestry seen between vertebrates we noticed that OXR genes from the zebrafish and OXR genes from human have a common architecture. Furthermore in both zebrafish and humans the small TLDc containing isoforms from LysM encoding genes cluster together but also cluster with small TLDc containing isoforms from *L82*. High sequence homology between human, zebrafish and fruitfly protein isoform sequences suggests a conserved protein function.

In humans the *LysMD1* locus is on Chr1 and expresses two different transcripts, composed of four exons coding two different proteins, of 227 aa and 179 aa. The longer isoform clusters with the zebrafish LysMD1 protein. In human the *LysMD2* is located on Chr15 and has two different transcripts composed of four exons, which encode two different proteins of 215 aa and 124 aa. The zebrafish and human full length LysMD2 proteins also cluster together. The *LysMD3* locus on human Chr5 is composed of five exons, alternatively spliced into four different transcripts corresponding to putative proteins of 127 aa, 150 aa and 306 aa. The fourth transcript, potentially encoding a 90 aa polypeptide, is suggested to undergo non-sense mediated decay, which is a cellular mechanism of mRNA surveillance that functions to detect non-sense mutations and prevent the expression of truncated or erroneous proteins (Chang et al., 2007). The *LysMD4* locus on human

Chr15 is composed of eight exons and gives rise to nine different transcripts. Two of those transcripts do not contain any open reading frame while two others contain intronic sequences and appear as non-coding transcripts. Five proteins of 297 aa, 296 aa, 296 aa, 170 aa and 123 aa are proposed to be products of the human *LysMD4*. The zebrafish LysMD3 and LysMD4 proteins cluster together, with the longest isoforms from human *LysMD3* and *LysMD4* in Fig. 2 panelA.

The human *OXR1* gene locus on Chr8, composed of 21 exons and at least 18 transcripts, are found in the human transcriptome. These transcripts code fifteen different OXR1 polypeptides. Two of the human *OXR1* transcripts are proposed to undergo non – sense mediated decay and three other transcripts are non-coding. The human *OXR2* is located on Chr6 and is composed of twenty exons. Fifteen alternatively spliced transcripts correspond with fourteen different OXR2 polypeptides. Despite significant sequence homology with their human orthologs the zebrafish OXR2 proteins cluster with OXR1 proteins in Fig. 2 panel B. Furthermore, supporting the hypothesis of an ancient duplication of OXR genes in zebrafish, we noticed that exons 13–18 of *OXR1* are encoding the same number of amino acids as exons 13–18 in *OXR2* (Fig. 1 panel B).

The minimal LysM domains from LysMD and OXR genes from zebrafish and human, were calculated and aligned for a phylogenetic pairwise comparison with LysM domains obtained from *D. Discoidum*, from fruit fly, and from *A. Thaliana* (Fig. 2, panel C). Sequence identity appears between the LysM domains studied. While a proline-glycine or even threonine-glycine (PG versus TG) is found at position 39–40 only in OXR LysM domains, the presence of lysine-arginine (KR in these vertebrates) or even from arginine-arginine (RR in a fruitfly LysMD) at position 25–26, characterizes the LysM domain from the LysMD genes in this analysis.

Homology is found between LysM domains from zebrafish and humans. The LysM domain encoded in *OXR2* clusters with the LysM domain encoded in *OXR1* in this analysis, which also supports the hypothesis of an ancient duplication event of OXR genes in zebrafish. In this study the LysM domain from *A. thaliana* CERK1 protein aligns with LysM domains from the OXR family (Fig. 2, panel C).

2.2. LysM gene response to bacteria in microarray experiments

The sensing activity of LysM-domain proteins of plants, toward pathogen associated molecular pattern molecules (PAMP) such as chitin type or structurally related molecules, (Zipfel, 2009) poses the question whether LysM-domain proteins can have a similar sensing function in animals. Therefore we searched published micro-array data sets to identify LysM gene responses in zebrafish embryos, or adults animals, infected with strains of *S. typhimurium* (Stockhammer et al., 2009) or *M. marinum* (Meijer et al., 2005; Van der Sar et al., 2009). Zebrafish *OXR* and LysMD probes (Fig. 1) were designed and analysed in several micro-array experiments. The data shows that zebrafish OXR and LysMD probes present on the micro-array platform do not respond to *Salmonella* (Stockhammer et al., 2009) or to *Mycobacterium* (Meijer et al., 2005) infection in zebrafish (Supplementary Table 2). These results contrast with the regulation of LysM domain encoding genes (*Lys* genes) induced in *L. japonicus* by the symbiotic *Mesorhizobium loti*, by chitin carbohydrates, or by both (Lohmann et al., 2010). However, *Salmonella* and *Mycobacteria* do not possess a thick layer of PG or chitin-like carbohydrates in their cell walls, and these ligands are often proposed for the LysM domain containing proteins. Therefore, the LysM genes response to PG, to chitin, or to structurally related molecules, remains to be investigated further in animals. In the absence of LysM genes response we decided to focus in more detail on the developmental expression patterns of the LysM domain containing families.

2.3. Spatio-temporal expression of LysMD and OXR genes in zebrafish embryos

2.3.1. Whole Mount In Situ hybridization expression patterns WISH

Preliminary RT-PCRs revealed high expression levels of the zebrafish LysMD genes and OXR genes in each of the early zebrafish embryonic developmental stages tested (from few cell stages to 12 hpf), in the *in situ* hybridization studies and also in adult animal RNA samples. As active zygotic expression is not considered to occur before the blastula stage these results suggest that LysM genes are highly expressed both maternally and zygotically in the zebrafish embryo. To investigate the spatio-temporal expression of these genes, whole mount *in situ* hybridization (WISH) was performed during early zebrafish embryogenesis. Developmental stages starting at the 1–4 cell stage, proceeding to sphere stage, shield stage, epiboly 90%, bud, 24 hpf, 48 hpf, 72 hpf and finally 5 dpf were analysed. The hybridization probes used were designed to regions outside of the LysM domain and, when possible, also outside of other homology domain positions. The probe positions in the LysM cDNAs are indicated in Fig. 1. Expression of all LysM genes was detected ubiquitously with WISH up to the bud stage (early zebrafish developmental stages shown in WISH Supplementary Fig. A), while the expression patterns in the CNS were first detected from 24 hpf in the embryos (Fig. 3, panel A: LysMD; Fig. 3, panel B: OXR).

The CNS patterns of the *LysMD1*, *LysMD2*, *LysMD3* and *LysMD4* from 24 hpf to 5 dpf is shown in Fig. 3 panel A. The *LysMD1* probe revealed an area of the brain strongly stained from 48 hpf to 5 dpf. This area stained in *LysMD1* expression pattern appeared similar to an area stained with the *LysMD4* probe; this brain structure remains unidentified in this study. From from 24 hpf to 5 dpf (Fig. 3, panel B) all OXR expression patterns show highest staining intensity in the zebrafish head and dorsal area.

The OXR1B/C probe also detected *OXR1* expression in two symmetrical series of cell clusters at the back of the zebrafish head, visible from the posterior axis. This unidentified pattern corresponds with cellular structures in the CNS. Furthermore we observed stained olfactory pits at 48 hpf with OXR1 B/C expression pattern (Fig. 3, panel B, 2 dpf). The OXR2 probes also revealed a strong expression of *OXR2* in the zebrafish forebrain and in the back of the brain (Fig. 3, panel B from 2 dpf).

2.3.2. Single fluorescent in situ hybridizations FISH and double ISH DISH

We decided to focus on *OXR1* and *OXR2* genes to study their expression patterns with fluorescent *in situ* hybridization (RNA FISH and RNA Double ISH) and high resolution laser scanning fluorescence confocal microscopy. Results at 24 hpf are presented in Fig 4 (FISH OXR), in Fig. 5 (DISH *OXR1*). Results at 48 hpf are shown in Fig. 6 (FISH OXR at 48 hpf) and in Supplementary Fig. E. The RNA FISH shows high expression levels of OXR in the CNS, more specifically in the brain of24 hpf and 48 hpf zebrafish embryos. These fluorescent expression patterns validate the previously observed CNS expression patterns detected with alkaline phosphatase detection. Technical validation and comparison of FISH and WISH for *MyoD1*, as a reference expression pattern, is shown in Supplementary Fig. B.

The specific expression pattern observed with OXR1B/C probe, in symmetrical cell clusters in the CNS, was also confirmed with RNA FISH (in Fig. 4, in Fig. 6 and in Fig. E). These structures were later identified (Fig. 9 and Fig. 10) as lateral line ganglia. Furthermore we focused on the olfactory pit (OP) region in the 48 hpf OXR1 B/C zebrafish embryo (Fig. 7 and Supplementary Fig. C). The OP contain chemo-sensitive cellular structures from the CNS. Confocal sections of the OP region are compared with WISH in Fig. 7. OXR2 expression was dominant in a distinctive forebrain region observed with RNA FISH (Fig. 6C), also confirming the CNS

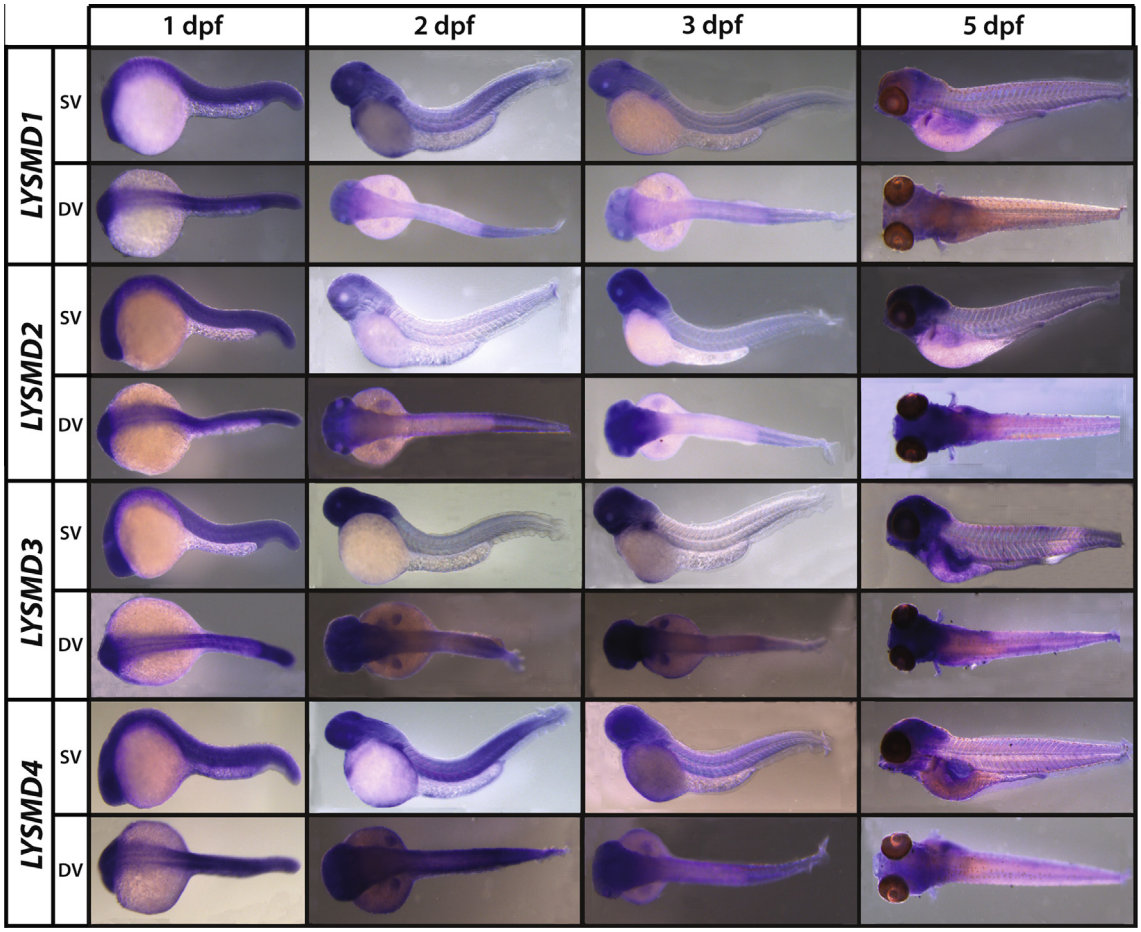

Fig. 3. LysMD (panel A) and OXR (panel B) genes expression patterns during stages of zebrafish development. Whole mount *in situ* hybrizations using alkaline phosphatase detection and a blue chromogenic substrate. Embryos are orientated with the anterior to the left and dorsal to the top and shown in side view (SV) or dorsal view (DV) at four developmental stages (1,2,3 and 5 dpf).

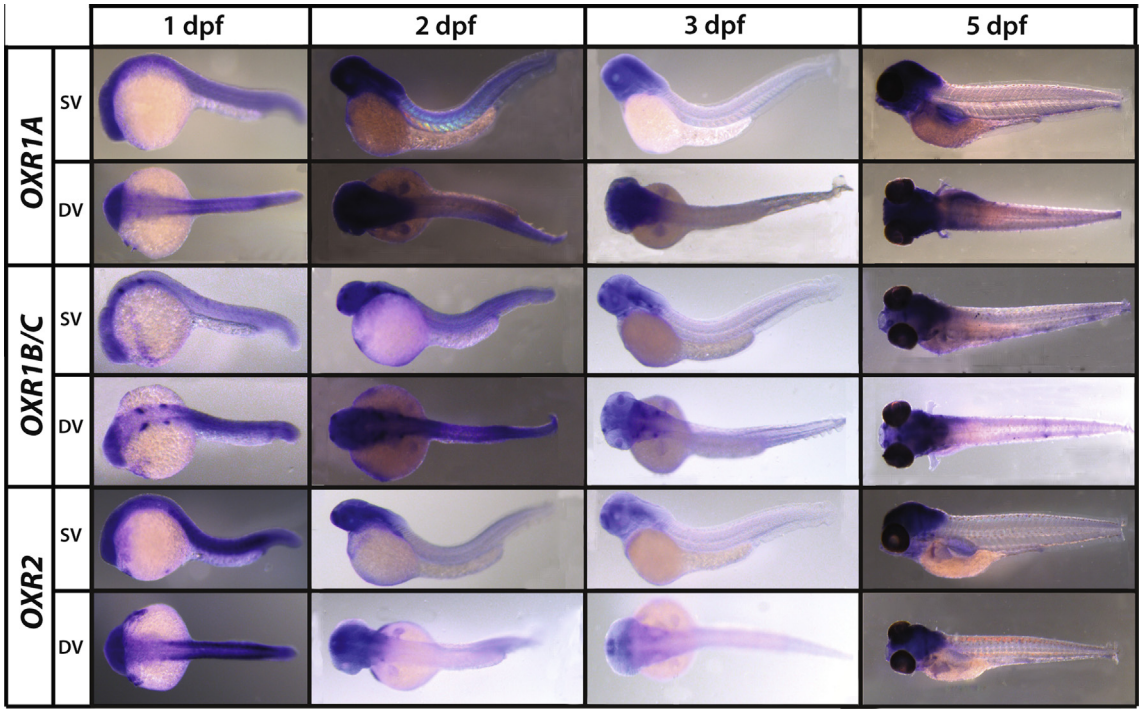

Fig. 3. (*continued*)

expression pattern previously detected using alkaline phosphatase detection (Fig. 3, Panel B, 2 dpf).

To investigate further we performed double fluorescence *in situ* hybridization (RNA DISH) to compare OXR1A and OXR1B probes patterns. The results from this approach revealed differential expression patterns for OXR1 splice variants probes A and probe B/C, in zebrafish embryos from 24 hpf (Fig. 5) but also at 48 hpf (DISH in Supplementary Fig. D). In both cases the OXR mRNA appeared differentially expressed in zebrafish CNS tissues. However it should be noticed that the OXR1A probe overlaps with all OXR genes transcripts and that this probe, located in the Ct coding region, might hybridize with other TLDc domain encoding transcripts (in essence from *OXR2* or from the TBC family).

To further illustrate *OXR* expression patterns confocal reconstructions movies from Z-series shown in Figs. 4–6, Fig. D and Fig. E are given in the Supplemental section (movies S1 to S13). The Supplementary movie S1 is an animated reconstruction of OXR1A and OXR1B/C DISH at 24 hpf showing different angles than the 2D images from Fig. 5. The Supplementary movies S2 (ventral view) and S3 (dorsal view) are animated reconstructions from DISH confocal acquisitions at 24 hpf showing ventral view which is not shown in Fig. 5. The Supplementary movies S4 (OXR1A), S5 (OXR1B/C) and S6 (OXR2) show animated reconstructions of OXR family from FISH at 24 hpf. The Supplementary movies S4, S5 and S6 present different observation angles than the 2D images from Fig. 4. The Supplementary movie S7 show OXR1A isoform expression pattern gradually through the *z*-axis of the 48 hpf zebrafish embryo and provides far more details than the 2D maximum overlay presented in Fig. 6. The movies S8 (OXR1A) and S9 (OXR1B) show animated reconstructions of *OXR1* expression patterns in 48 hpf zebrafish embryos that can be observed from different angles than the 2D maximum overlays from Fig. 6. The movies S10 (*OXR2* side view) and S11 (*OXR2* dorsal view) show *OXR2* expression pattern in 48 hpf zebrafish embryos from different perspectives than the images in Fig. 6 and in Supplementary Fig. E. The movies S12 (side view) and S13 (dorsal view) show animated reconstruction from OXR1A and OXR1B/C merged channel DISH in 48 hpf zebrafish embryos. The movies S12 and S13 provide additional observation angles of *OXR1* expression patterns than the 2D images from Fig. D.

To further study the unidentified cellular structures in the zebrafish CNS we have analysed WISH, FISH and microtome sections. Representative WISH microsections and laser scanning confocal stacks from *OXR1* and *OXR2* RNA FISH and WISH are compared in Fig. 8. A micro-section of OXR1 B/C stained zebrafish head is compared with WISH and FISH (Fig. 8A1–A3) and shows expression pattern in zebrafish OP. OXR2 appears expressed in a distinctive forebrain region and micro-section of OXR2 stained zebrafish brain is also compared with WISH and FISH expression pattern at 48 hpf (Fig. 8, B1–B3).

2.3.3. Modelling OXR expression in zebrafish brain atlas

In order to identify the brain regions corresponding with OXR expression pattern in zebrafish we decided to use the FISH data sets to create three dimensional models. The OXR models were integrated into software dedicated to the zebrafish atlas (Potikanond and Verbeek, 2011) for a comparison. The 3D models were generated from the confocal laser scanning microscope stacks obtained from the FISH (Welten et al., 2006). Per optical slice, the areas with high signal were delineated as areas of gene expression. This is realized with dedicated annotation software and the result is an annotated 3D model that can be visualized (Potikanond and Verbeek, 2011) and compared with patterns obtained from gene markers that have already been mapped. In this manner the relationship between expression patterns can be established by semantics relations, by relations obtained from machine learning, or by spatial mapping (M. and FJ. (2008). Data Integration for Spatio-Temporal Patterns of Gene Expression of Zebrafish develop-

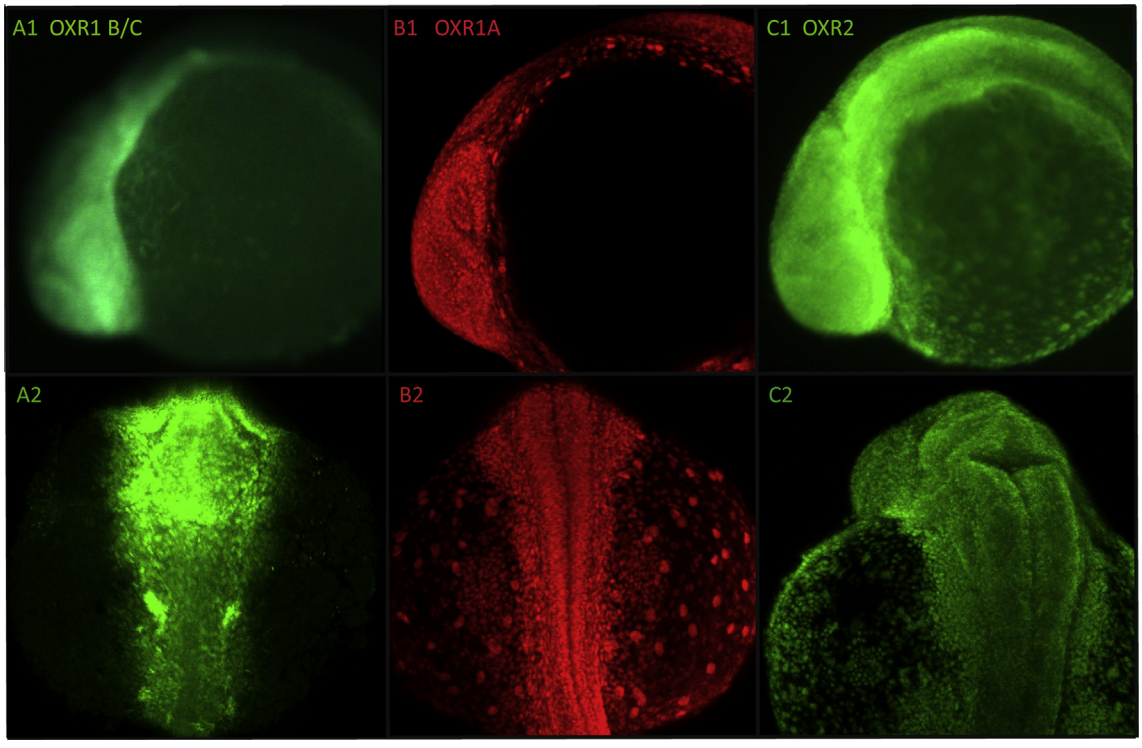

Fig. 4. Expression patterns of OXR genes with FISH in 24 hpf zebrafish embryos. The images are maximum intensity projections from confocal z-series of OXR1B/C (fluorescein green, in A1, A2), OXR1A (Cy3 red in B1, B2) and OXR2 (fluorescein green, in C1, C2). The embryos (A1, B1, C1) are orientated with the anterior to the left and the embryos (A2, B2, C2) are orientated with the anterior to the top and shown in dorsal view.

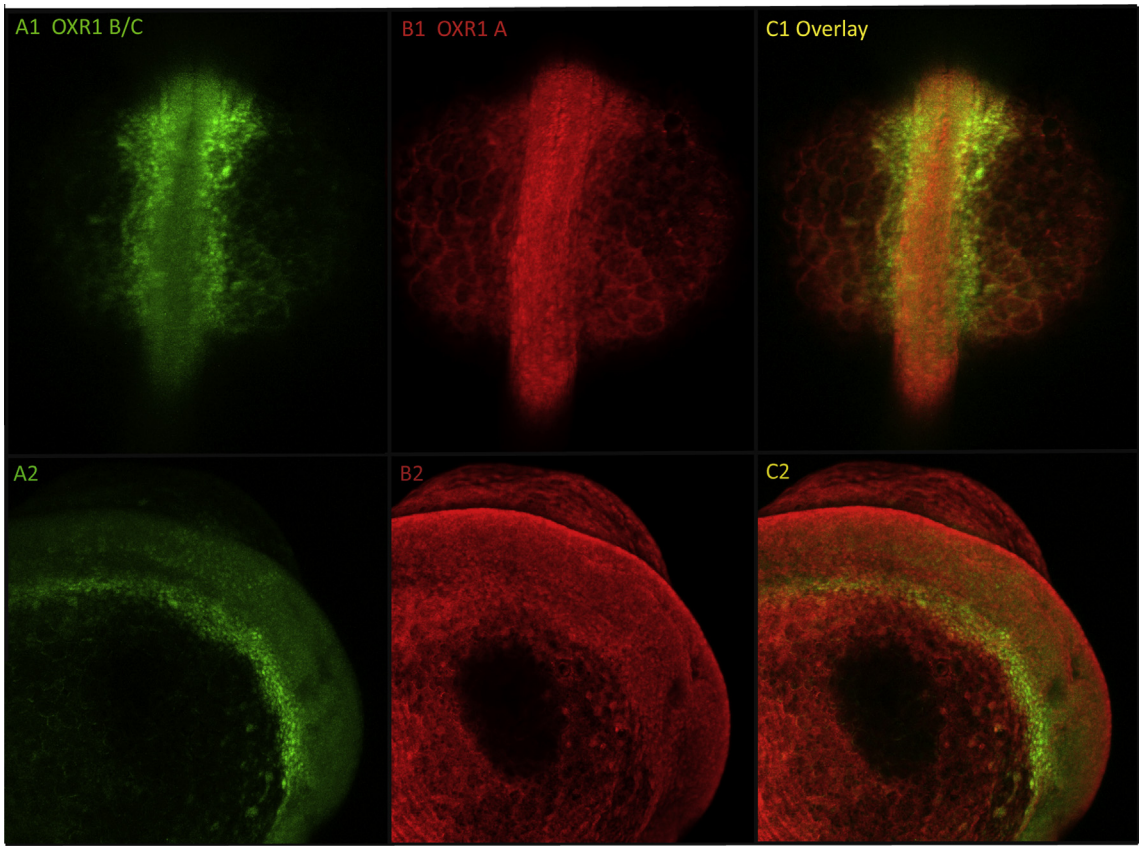

Fig. 5. The expression patterns of OXR1A and OXR1B/C in 24 hpf zebrafish embryo with double *in situ* hybridizations (DISH). The images are maximum intensity projections from dual channel confocal z-series. OXR1B/C is shown in green (fluorescein, A1, A2). OXR1A is shown in red (Cy3 dye, B1, B2). The merged channels from OXR1B/C and OXR1A are shown in yellow (C1, C2) for a comparison. The embryo (A1, B1, C1) is orientated with the anterior to the top and shown in dorsal view. The same embryo (A2, B2, C2) is orientated with the anterior to the right and shown in side view.

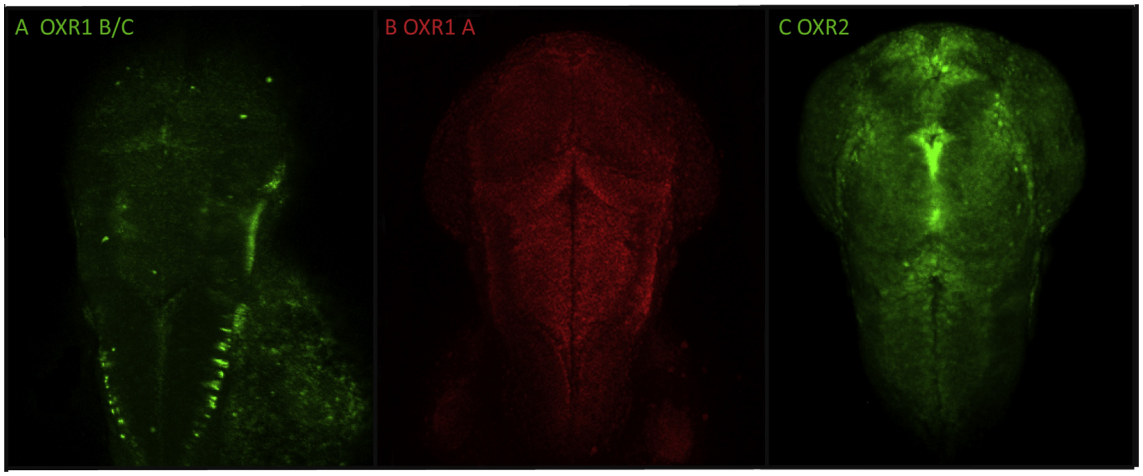

Fig. 6. OXR1 and OXR2 RNA FISH expression patterns at 48 hpf in zebrafish embryos. The images are maximum intensity projections from laser scanning confocal z-series of OXR1B/C (fluorescein, A), OXR1A (Cy3, B) and OXR2(Fluorescein, C). The embryos are orientated with the anterior to the top and presented in dorsal view.

ment: the GEMS database). The resulting 3D models for the LysM gene are depicted in Fig. 9 and can be compared with the 3D zebrafish atlas (Verbeek et al., 2002) (http://bio-imaging.liacs.nl/ZFAtlasServer) and with other patterns and markers that have already been mapped (Belmamoune et al., 2010). Co-localization analyses with the marker gene Dlx5a, a homeobox gene involved in craniofacial development in several vertebrates, shows that the zebrafish *OXR1* B/C expression pattern can be attributed to the olfactory bulb region Fig. 10. The olfactory bulbs are forebrain symmetrical structures connected with OP and involved in olfaction. In addition co-localization with the marker gene *14-3-3* γ isoform abundantly expressed in the CNS indicates that *OXR1* also localizes to the lateral line ganglia in zebrafish. The lateral line ganglions develop from a cranial ectodermal placode and contain sensory neurons that innervate the posterior lateral line system. More detailed 3D models can be visualized and compared on the web site of the zebrafish

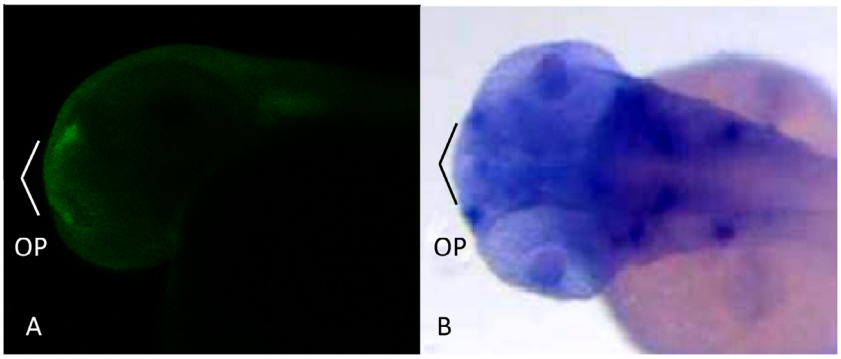

Fig. 7. OXR1 B/C expression in the olfactory pits of zebrafish embryos at 48 hpf. FISH and WISH comparison (A) Maximum intensity projection of stacks, covering ~20 μM, from fluorescein Z-series OXR1B/C at 48 hpf (B) WISH OXR1 B/C at 48 hpf. Embryos are orientated with the anterior to the left and shown in side view (A) or dorsal view (B).

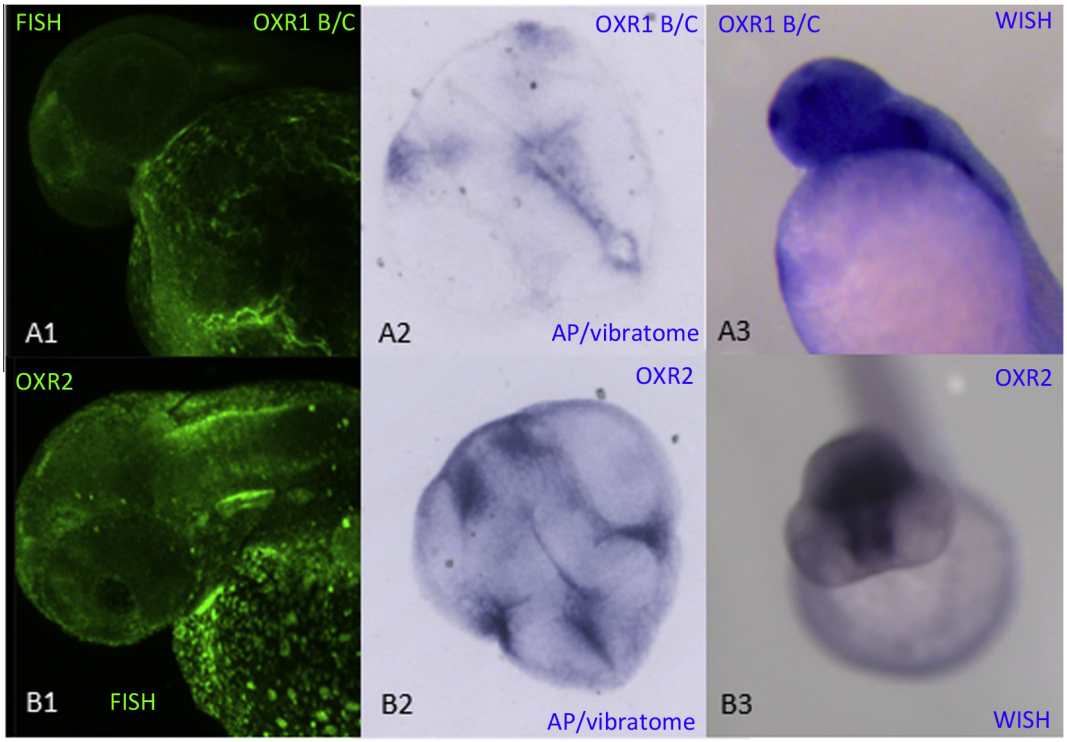

Fig. 8. OXR1 and OXR2 expression in 48 hpf zebrafish embryo brain. The WISH and FISH expression pattern are compared with representative brain micro-sections. (A1) Maximum intensity projection from fluorescein confocal z-series of OXR1 B/C. (A2) OXR1 B/C transversal 6 μm thick section (A3) OXR1 B/C WISH (B1) maximum intensity projection of OXR2 fluorescein confocal z-series (B2) OXR2 transversal 6 μm thick section, (A3) OXR2 WISH for a comparison. The embryos (A1, B1, A3) are orientated with anterior to the left and shown in side view. Embryo (B3) is orientated with the anterior to the back and shown in frontal view.

atlas (http://bioimaging.liacs.nl/liacsatlas.html). In the future we have hope that many more gene markers will be available in the zebrafish atlas thus allowing further comparisons and analysis of the LysM encoding genes expression patterns.

3. Experimental materials and methods

3.1. In silico methods

The ENSEMBL, NCBI and VEGA genome browsers were mined for LysM encoding genes using the LysM domain consensus sequence of 44 amino acids that was obtained from Pfam entry PF01476. The NCBI Conserved Domain Database (CDD) was searched for zebrafish LysM gene homologs. BLAST and TBLASTN were performed on the ZV9 release of the zebrafish EMSEMBL genome browser. The pairwise alignments and phylogenetic trees were generated using CLC DNA workbench 6 (http://www.clcbio.com) and sequences from organism other than *Danio Rerio* were obtained from ENSEMBL or FlyBase genome browsers.

The Small Modular Architecture Tool (SMART) (http://smart.embl-heidelberg.de) was used for protein domain predictions and taxonomic distribution. The TransMembrane Hidden Markov Model TMHMM (http://www.cbs.dtu.dk/services/TMHMM-2.0) and TopPRED 0.01 (http://mobyle.pasteur.fr/cgi-bin/portal.py?#forms::toppred) were used to refine prediction of a transmembrane helix in proteins.

3.2. Animal handling and fixation

Zebrafish albinos (fluorescence) or ABxTL (alkaline phosphatase) embryos were handled in compliance with local animal care

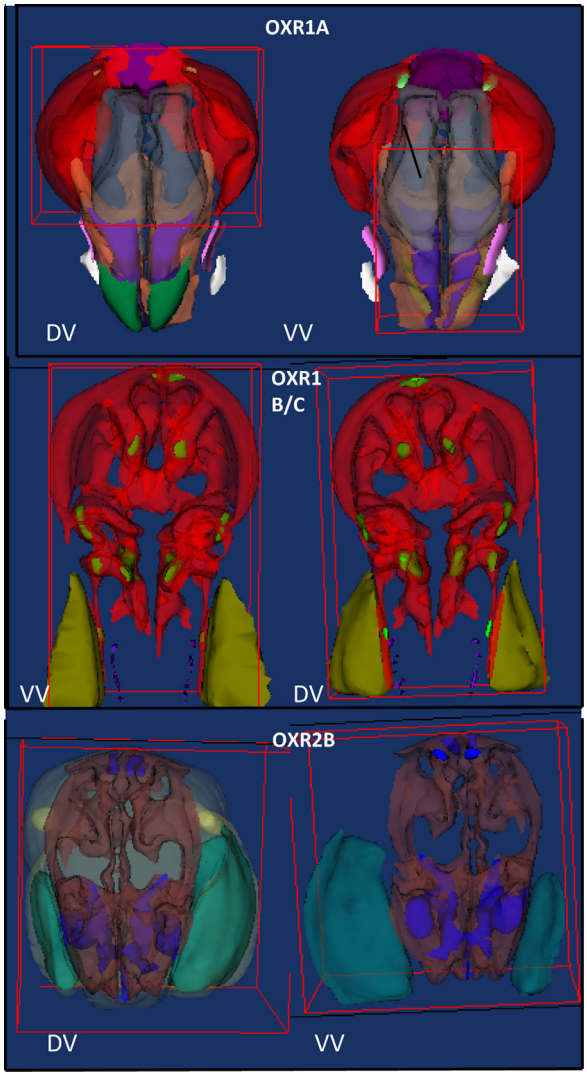

Fig. 9. Three dimension modeling representing OXR FISH expression pattern in 48 hpf zebrafish embryos. (A-B-C) The 3D models were rebuilt from CSLM stacks redrawn by hands on LCD tablet using the TDR-base software. The OXR1A (A), the OXR1 B/C (B) and the OXR2 (C) expression patterns were reconstructed for integration into the zebrafish embryo brain atlas. The 3D models are presented with the anterior to the top and shown in dorsal view (1) and in ventral view (2). In these models, the colors are arbitrarily attributed by levels of signal intensity. (red/brown/pink) area of signal, (greens) strong signal (purple/blue) very strong signal, (yellow/turquoise) zebrafish yolk as a reference.

regulations. Several stages of zebrafish embryonic development were selected; few cell stages, oblong to sphere, shield, epiboly 80–90%, 24 h post fertilization (hpf), 48 hpf, 72 hpf and 5 days post fertilization (dpf) and either collected for RNA extraction and cloning sequencing purposes or for whole mount *in situ* hybridization.

The embryos were either flash freezed in LN_2, in phenol, and immediately stored at −80 °C for further nucleic acids extraction or directly fixed overnight in Phosphate Buffer Saline/Tween20 0,1% /Paraformaldehyde 4% (PBST-PFA) for *in situ* hybridizations. Zebrafish chorions were removed by hands.

3.3. Cloning

Whole nucleic acid extracts were prepared from ~50 embryos staged, crushed in phenol/chloroform, ethanol washed and briefly dried under a clean fume hood before resuspension in nuclease free water containing RNAse inhibitor (*RNAse OUT, Invitrogen,* Carlsbad, CA). Whole RNA extracts were obtained after treatment with *Ambion DNA free* kit (*Applied biosystems*).

All RT-PCR amplifications were performed using *SuperscriptIII high fidelity* (*Invitrogen,* Carlsbad, CA) kit and cDNAs were obtained after 30 min retro-transcription at 55 °C and 35 cycles of PCR amplification. Primers Tm were homogenized at 60 °C using Primer3 (http://frodo.wi.mit.edu/primer3) and polymer sequences are given in Supplementary Table 1.

LysM encoding cDNAs bands were excised from agarose gel with a single use n°10 sharp carbon steel surgical blade (*Swann-Morton, LTD)* and purified using *High pure PCR cleanup* kit (*Roche Diagnostics*) for blunt cloning into the *PCR4* vector with *Zero blunt TOPO kit for sequencing* (*Invitrogen, Carlsbad, CA*). Blunt cloning OXR2B cDNA product required 2 rounds of excision/RT-PCR re-amplification.

3.4. Ribonucleoprobes design and synthesis

Specific regions inside each LysM cDNA were flanked with primer pairs containing the T3 and T7 promoting sequences overhang for sense or antisense probe synthesis. The PCR4 blunt plasmid constructions were used as templates and amplified products were purified using *High Pure PCR Cleanup Micro Kit* (*Roche diagnostics*). *In vitro* transcriptions were performed with *Ambion* T7 *MAXISCRIPT* kit (*Applied Biosystems*) for probe synthesis and either DIG labeled ribonucleotides or fluorescein labeled ribonucleotides (*Roche Diagnostics*) were used for the synthesis reactions. Ribonucleoprobes were purified by precipitation overnight in glycogen, ammonium

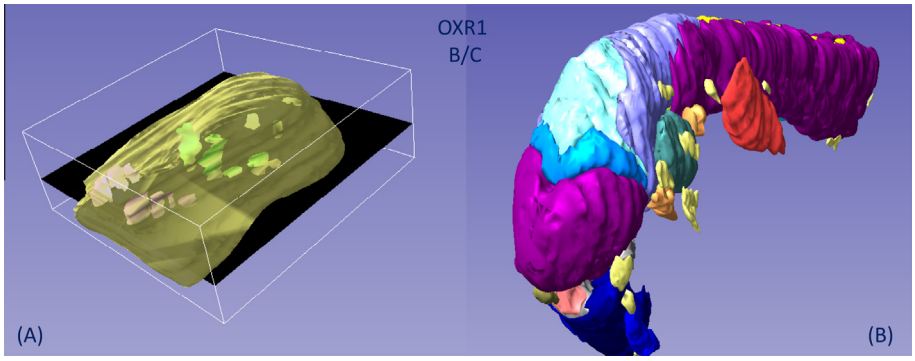

Fig. 10. OXR1 B/C expression pattern modeling in 48 hpf zebrafish embryos. (A) TDR 3D/base output for OXR1B/C showing co-localization with *14-3-3* γ isoform and DLX5a expression patterns. (B) Partial display of annotated structures in the zebrafish atlas. Annotated structures from neuro-tissues, according to the zebrafish atlas (http://bio-imaging.liacs.nl/ZFAtlasServer). For reference the fin buds are also displayed: (dark Blue) telencephalon-diencephalon; (Pink) third ventricle; (Purple) mesencephalon; (Cyan) fourth ventricle; (Light blue) myelencephalon, (Turquoise) rombencephalon; (Yellow) lateral line neurons; (Purple) somites; (Red) Pectoral Fin bud; [Yellow (in somites)] spinal chord.

acetate and ethanol, then resuspended in nuclease free water containing RNAse inhibitor.

3.5. WISH, FISH and DISH

PFA fixed embryos were whitened in methanol and permeabilized with Proteinase K. Whole Mount *In Situ* Hybridizations were performed as previously described (Meijer et al., 2005) for microsection or for expression pattern characterization. Blocking of the zebrafish embryos was done in *western blotting blocking reagent* (*Roche Diagnostics*) supplemented with 2% sheep serum for 3 h. The conjugated alkaline phosphatase sheep-anti-DIG antibody (*Roche Diagnostics*) was used at 1/3000 dilution overnight at 4 °C. Staining was monitored at room temperature for 1–8 h in the presence of either *BMP purple* or *NBT/BCIP* (*Roche Diagnostics*) chromogenic substrates. The WISH were observed on a LEICA stereo MS5.

Single and double fluorescence *In Situ* Hybridizations (RNA FISH and RNA DISH) were performed using either sheep-anti-DIG or sheep-anti-fluorescein primary antibodies at 1/3000 dilution overnight at 4 °C, followed by incubation with HRP-conjugated anti-sheep secondary antibody at 1/200 dilution overnight at 4 °C. Quenching of endogenous peroxidase and HRP (for DISH) were performed sequentially using 3% H_2O_2 in PBT. Fluorescent expression patterns were revealed with TSA-plus fluorescein or TSA-plus Cyanine3 system kit (*Perkin Elmer LAS*). Embryos were screened with a Leica MZ16FA stereo fluorescent microscope and respectively observed at 488 nm or 543 nm on a Zeiss LSM5 Exciter/AxioImager confocal microscope.

For imaging purposes the WISH embryos were immobilized in Methyl cellulose 1.5%. Alternatively, for RNA FISH and laser scanning fluorescence confocal microscopy, embryos were mounted in a 1.5% low melting agarose gel (*Marinagar*).

3.6. Micro-sections

The 48 hpf embryos were fixed in 4% PFA/PBT for 30 min and dehydrated in ethanol overnight. The embryos were then washed in ethanol/Histo-resin before embedding in Histo-resin (*Leicabiosystems*) according to manufacturer instructions. Transversal 6-μm-thick sections were obtained with a microtome.

3.7. 3D modeling

The images (stacks obtained from confocal laser scanning microcopy) were redrawn by hand and relevant anatomical parts were annotated, with a LCD tablet, next to the areas of gene expression. The annotated images were assembled and analysed with our annotation software (Lohmann et al., 2010; Welten et al., 2006) (TDR-3Dbase). The result was visualized (Potikanond and Verbeek, 2011, 2002) with our annotation software (TDR-3Dbase).

Acknowledgements

We thank the CARB centre, the Danish National Research Foundation, Aarhus University (AU), grant No. DNRF79 and Leiden University Biology Institute (IBL) for financial support. We thank Saskia Rueb for technical expertise. We thank Ulrike Nehrdich and Davy De Witt for the zebrafish care and maintenance. We are very grateful to Fleur-Catherine Dolman for her kind help with this manuscript.

Appendix A. Supplementary data

Supplementary data associated with this article can be found, in the online version, athttp://dx.doi.org/10.1016/j.gep.2013.02.007.

References

Buist, G., Steen, A., Kok, J., Kuipers, O.P., 2008. LysM, a widely distributed protein motif for binding to (peptido)glycans. Mol. Microbiol. 68 (4), 838–847, Review.
Steen, A., Buist, G., Horsburgh, G.J., Venema, G., Kuipers, O.P., Foster, S.J., Kok, J., 2005 Jun. AcmA of *Lactococcus lactis* is an N-acetylglucosaminidase with an optimal number of LysM domains for proper functioning. FEBS J. 272 (11), 2854–2868.
Madsen, E.B., Madsen, L.H., Radutoiu, S., Olbryt, M., Rakwalska, M., Szczyglowski, K., Sato, S., Kaneko, T., Tabata, S., Sandal, N., Stougaard, J., 2003. A receptor kinase gene of the LysM type is involved in legume perception of rhizobial signals. Nature 425 (6958), 637–640.
Radutoiu, S., Madsen, L.H., Madsen, E.B., Felle, H.H., Umehara, Y., Grønlund, M., Sato, S., Nakamura, Y., Tabata, S., Sandal, N., Stougaard, J., 2003. Plant recognition of symbiotic bacteria requires two LysM receptor-like kinases. Nature 425 (6958), 585–592.
Radutoiu, S., Madsen, L.H., Madsen, E.B., Jurkiewicz, A., Fukai, E., Quistgaard, E.M., Albrektsen, A.S., James, E.K., Thirup, S., Stougaard, J., 2007. LysM domains mediate lipochitin-oligosaccharide recognition and Nfr genes extend the symbiotic host range. EMBO J. 26 (17), 3923–3935.
Broghammer, A., Krusell, L., Blaise, M., Sauer, J., Sullivan, J.T., Maolanon, N., Vinther, M., Lorentzen, A., Madsen, E.B., Jensen, K.J., Roepstorff, P., Thirup, S., Ronson, C.W., Thygesen, M.B., Stougaard, J., 2012. Legume receptors perceive the rhizobial lipochitin oligosaccharide signal molecules by direct binding. Proc. Natl. Acad. Sci. USA 109 (34), 13859–13864. http://dx.doi.org/10.1073/pnas.1205171109. Epub 2012 Aug 2.
Wan, J., Zhang, X.C., Neece, D., Ramonell, K.M., Clough, S., Kim, S.Y., Stacey, M.G., Stacey, G., 2008. A. LysM receptor-like kinase plays a critical role in chitin signaling and fungal resistance in *Arabidopsis*. Plant Cell 20 (2), 471–481.
Miya, A., Albert, P., Shinya, T., Desaki, Y., Ichimura, K., Shirasu, K., Narusaka, Y., Kawakami, N., Kaku, H., Shibuya, N., 2007. CERK1, a LysM receptor kinase, is essential for chitin elicitor signaling in *Arabidopsis*. Proc. Natl. Acad. Sci. USA 104 (49), 19613–19618.
Shimizu, T., Nakano, T., Takamizawa, D., Desaki, Y., Ishii-Minami, N., Nishizawa, Y., Minami, E., Okada, K., Yamane, H., Kaku, H., Shibuya, N., 2010. Two LysM receptor molecules, CEBiP and OsCERK1, cooperatively regulate chitin elicitor signaling in rice. Plant J. 64 (2), 204–214, 10.1111/j.1365-313X.2010.04324.
de Jonge, R., van Esse, H.P., Kombrink, A., Shinya, T., Desaki, Y., Bours, R., van der Krol, S., Shibuya, N., Joosten, M.H., Thomma, B.P., 2010. Conserved fungal LysM effector Ecp6 prevents chitin-triggered immunity in plants. Science 329 (4), 953–955.
Willmann, Heini M. Lajunen, Gitte Erbs, Mari-Anne Newman, Dagmar Kolb, Kenichi Tsuda, Fumiaki Katagiri, Judith Fliegmann, Jean-Jacques Bono, Julie V. Cullimore, Anna K. Jehle, Friedrich Götz, Andreas Kulik, Antonio Molinaro, Volker Lipka, Andrea A. Gust, Thorsten Nürnberger. (2012). Arabidopsis Lysin-motif proteins LYM1 LYM3 CERK1 mediate bacterial peptidoglycan sensing and immunity to bacterial infection. Proc Natl Acad Sci U S A. 108 (49) (2011) 19824–19829 (Published online 2011 November 21. doi: 10.1073/pnas.1112862108).
Volkert, M.R., Elliott, N.A., Housman, D.E., 2000. Functional genomics reveals a family of eukaryotic oxidation protection genes. Proc Natl Acad Sci U S A. 97 (26), 14530–14535.
Durand, M., Kolpak, A., Farrell, T., Elliott, N.A., Shao, W., Brown, M., Volkert, M.R., 2007. The OXR domain defines a conserved family of eukaryotic oxidation resistance proteins. BMC Cell Biol. 8 (2007), 13.
Oliver, P.L., Finelli, M.J., Edwards, B., Bitoun, E., Butts, D.L., Becker, E.B., Cheeseman, M.T., Davies, B., Davies, K.E., 2011. Oxr1 is essential for protection against oxidative stress-induced neurodegeneration. PLoS Genet. 7 (10), e1002338.
Shao, W., Halachmi, S., Brown, M., 2002. ERAP140, a conserved tissue-specific nuclear receptor coactivator. Mol Cell Biol. 22 (10), 3358–3372.
Kinyamu, H.K., Collins, J.B., Grissom, S.F., Hebbar, P.B., Archer, T.K., 2008. Genome wide transcriptional profiling in breast cancer cells reveals distinct changes in hormone receptor target genes and chromatin modifying enzymes after proteasome inhibition. Mol. Carcinog. 47 (11), 845–885.
Heemers, H.V., Regan, K.M., Schmidt, L.J., Anderson, S.K., Ballman, K.V., Tindall, D.J., 2009. Androgen modulation of coregulator expression in prostate cancer cells. Mol. Endocrinol. 23 (4), 572–583.
Arai, H., Ozaki, T., Niizuma, H., Nakamura, Y., Ohira, M., Takano, K., Matsumoto, M., Nakagawara, A., 2008. (2008) ERAP140/Nbla10993 is a novel favorable prognostic indicator for neuroblastoma induced in response to retinoic acid. Oncol. Rep. 19 (6), 1381–1388.
Higginbotham, K.S., Breyer, J.P., Bradley, K.M., Schuyler, P.A., Plummer Jr, W.D., Freudenthal, M.E., Trentham-Dietz, A., Newcomb, P.A., Sanders, M.E., Page, D.L., Parl, F.F., Egan, K.M., Dupont, W.D., Smith, J.R., 2011. A multistage association study identifies a breast cancer genetic locus at NCOA7. Cancer Res. 71 (11), 3881–3888.
Middleton, F.A., Pato, M.T., Gentile, K.L., Morley, C.P., X. Zhao, Eisener, A.F., Brown, A., Petryshen, T.L., Kirby, A.N., Medeiros, H., Carvalho, C., Macedo, A., Dourado, A., Coelho, I., Valente, J., Soares, M.J., Ferreira, C.P., Lei, M., Azevedo, M.H., Kennedy, J.L., Daly, M.J., Sklar, P., Pato, C.N., 2004. Genomewide linkage analysis of bipolar disorder by use of a high-density single-nucleotide-polymorphism

(SNP) genotyping assay: a comparison with microsatellite marker assays and finding of significant linkage to chromosome 6q22. Am. J. Hum. Genet. 74 (5), 886–897.

Pato, C.N., Middleton, F.A., Gentile, K.L., Morley, C.P., Medeiros, H., Macedo, A., Azevedo, M.H., Pato, M.T., 2005. Genetic linkage of bipolar disorder to chromosome 6q22 is a consistent finding in Portuguese subpopulations and may generalize to broader populations. Am. J. Med. Genet. B Neuropsychiatr. Genet. 134B (1), 119–121.

Liu, Y., Shi, Y., Guo, T., Gao, J., Qin, W., Li, S., Tang, W, Feng, G., Zhu, S., Liu, H., He, L., 2007. No association between the Nuclear Receptor Coactivator 7 gene and schizophrenia in the Chinese Han population. Schizophr. Res. 89 (1–3), 360–361.

Engels, H., Wohlleber, E., Zink, A., Hoyer, J., Ludwig, K.U., Brockschmidt, F.F., Wieczorek, D., Moog, U., Hellmann-Mersch, B., Weber, R.G., Willatt, L., Kreiss-Nachtsheim, M., Firth, H.V., Rauch, A., 2009. A novel microdeletion syndrome involving 5q14. 3-q15: clinical and molecular cytogenetic characterization of three patients. Eur J Hum Genet. 17 (12), 1592–1599.

Thisse, B., Heyer, V., Lux, A., Alunni, V., Degrave, A., Seiliez, I., Kirchner, J., Parkhill, J.P., Thisse, C., 2004. Spatial and temporal expression of the zebrafish genome by large-scale in situ hybridization screening. Methods Cell Biol. 77 (2004), 505–519.

Alsarraf HM, Laroche FJF, Spaink H, Thirup S, Blaise M. (2011). Purification, crystallization and preliminary crystallographic studies of the TLDc domain of oxidation resistance protein 2 from zebrafish. Acta Crystallogr Sect F Struct Biol Cryst Commun. 67 (Pt 10) (2011) 1253–6.

Blaise M, Alsarraf HM, Wong JEMM, Midtgaard SR, Laroche FJF, Schack L, Spaink HP, Stougaard J and Thirup S. (2012). Crystal structure of the TLDc domain of Oxidation resistance protein 2 from Zebrafish. Protein (2012). In press.

Doerks, T., Strauss, M., Brendel, M., Bork, P., 2000. GRAM, a novel domain in glucosyltransferases, myotubularins and other putative membrane-associated proteins. Trends Biochem Sci. 25 (10), 483–485.

Stowers, R.S., Russell, S., Garza, D., 1999. The 82F late puff contains the L82 gene, an essential member of a novel gene family. Dev. Biol. 213 (1), 116–130.

Wang Z, Berkey CD, Watnick PI. (2012). The Drosophila protein mustard tailors the innate immune response activated by the immune deficiency pathway. J Immunol. 2012 Apr 15;188(8):3993–4000. Epub 2012 Mar 16.

Jaramillo-Gutierrez G, Molina-Cruz A, Kumar S, Barillas-Mury C. (2010). The Anopheles gambiae oxidation resistance 1 (OXR1) gene regulates expression of enzymes that detoxify reactive oxygen species. PLoS One. 2010 Jun 17;5(6):e11168.

Chang YF, Imam JS, Wilkinson MF. (2007). The nonsense-mediated decay RNA surveillance pathway. Annu Rev Biochem. 2007; 76:51–74. Review.

Zipfel C. (2009). Early molecular events in PAMP-triggered immunity. Curr Opin Plant Biol. 2009 Aug; 12(4):414–20.

Stockhammer OW, Zakrzewska A, Hegedûs Z, Spaink HP, Meijer AH. (2009). Transcriptome profiling and functional analyses of the zebrafish embryonic innate immune response to Salmonella infection. J Immunol. 2009 May 1; 182 (9):5641–53.

Meijer AH, Verbeek FJ, Salas-Vidal E, Corredor-Adámez M, Bussman J, van der Sar AM, Otto GW, Geisler R, Spaink HP. (2005). Transcriptome profiling of adult zebrafish at the late stage of chronic tuberculosis due to Mycobacterium marinum infection. Mol Immunol. 2005 Jun; 42 (10):1185–203.

Van der Sar AM, Spaink HP, Zakrzewska A, Bitter W, Meijer AH. (2009). Specificity of the zebrafish host transcriptome response to acute and chronic mycobacterial infection and the role of innate and adaptive immune components. Mol Immunol. 2009 Jul; 46 (11–12):2317–32.

Lohmann GV, Shimoda Y, Nielsen MW, Jørgensen FG, Grossmann C, Sandal N, Sørensen K, Thirup S, Madsen LH, Tabata S, Sato S, Stougaard J, Radutoiu S. (2010). Evolution and regulation of the Lotus japonicus LysM receptor gene family. Mol Plant Microbe Interact. 2010 Apr; 23 (4):510–21.

Welten M.C.M., De Haan S, van den Boogert N, Noordermeer J.N., Lamers G, Spaink H.P., Meijer A.H., Verbeek FJ (2006) ZebraFISH: Fluorescent in situ hybridization protocol and 3D images of gene expression patterns. Zebrafish, Vol 3. #4, pp 465–476.

Potikanond, D., Verbeek, F.J., 2011. 3D Visual Integration of Spatio-Temporal Gene Expression Patterns on Digital Atlas of Zebrafish Embryo using Web Services. Proceedings Int. Conf. Advances in Communication and Information Technology (CIT 2011). Amsterdam 2011, 56–62.

Verbeek, F.J., Boon, P.J., Sloetjes, H., van der Velde, R., de Vos, N., 2002. Visualization of complex data sets over Internet: 2D and 3D visualization of the 3D digital atlas of zebrafish development. *Proceedings SPIE 4672*. Internet Imaging III, 20–29.

Belmamoune M. and Verbeek FJ. (2008). Data Integration for Spatio-Temporal Patterns of Gene Expression of Zebrafish development: the GEMS database. Journal of Integrative, BioInformatics, 5(2):92, 2008.

Belmamoune M, Potikanond D, Verbeek FJ. (2010). Mining and analysing spatio-temporal patterns of gene expression in an integrative database framework. Journal of Integrative, Bioinformatics, 7(3):128, 1–10, 2010.

Murphy KC, Volkert MR. Structural/functional analysis of the human OXR1 protein: identification of exon 8 as the anti-oxidant encoding function (2012). BMC Mol Biol. 2012; 13: 26. Published, online 2012 August 8. doi: 10.1186/1471-2199-13-26.

Tsujita, K., Itoh, T., Ijuin, T., Yamamoto, A., Shisheva, A., et al., 2004. Myotubularin regulates the function of the late endosome through the gram domain-phosphatidylinositol 3,5-bisphosphate interaction. J Biol Chem. 2004 (279), 13817–13824.